HOKKAIDO UNIVERSITY

Title	A novel murine model of idiopathic pulmonary fibrosis with persistent and marked features using Yama mice
Author(s)	Ramandani, Dhasia; Hasegawa, Moe; Yamada, Yusuke et al.
Citation	Japanese Journal of Veterinary Research, 74(1), 1-12 https://doi.org/10.57494/jjvr.74.1_1
Issue Date	2026-03-10
Doc URL	https://hdl.handle.net/2115/99039
Type	departmental bulletin paper
File Information	JJVR74-1_1-12_DhasiaRamandani.pdf

Hokkaido University Collection of Scholarly and Academic Papers : HUSCAP

Japanese Journal of Veterinary Research 74(1): 1–12, 2026

JJVR

REGULAR PAPER Experimental Research

A novel murine model of idiopathic pulmonary fibrosis with persistent and marked features using Yama mice

Dhasia Ramandani[1,2)], Moe Hasegawa[1)], Yusuke Yamada[1)], Kyoko Yoshizaki[1)], Masashi Sakurai[1)] and Masahiro Morimoto[1,*)]

[1)] Laboratory of Veterinary Pathology, Joint Faculty of Veterinary Medicine, Yamaguchi University, Japan
[2)] Department of Bioresources Technology and Veterinary, Vocational College, Universitas Gadjah Mada, Indonesia

Received for publication, November 5, 2025; accepted, November 26, 2025

Abstract

Idiopathic pulmonary fibrosis (IPF) is a chronic, progressive interstitial lung disease characterized by excessive collagen deposition and irreversible scarring. Reliable animal models are essential for elucidating IPF pathogenesis and evaluating antifibrotic therapies. However, conventional bleomycin (BLM) models generally induce only transient and moderate fibrosis. Considering the profibrotic role of eosinophils, we developed a novel IPF model using the spontaneous eosinophilic mutant Yama mice strain to achieve persistent and severe fibrosis. Male Yama and C57BL/6 mice (6 weeks old, n = 24) received eight intranasal administrations of BLM (2 mg/kg) at two-week intervals, while controls received saline. Peripheral eosinophil counts were monitored, and tissues were analyzed histologically and biochemically. Yama mice exhibited a sharp eosinophil peak after the first BLM exposure, followed by a gradual decline. Histological analysis revealed markedly enhanced fibrosis, greater collagen deposition, and higher Ashcroft scores in Yama mice than in C57BL/6 mice. Alcian blue–PAS-positive fibroblast foci, a characteristic feature of human IPF, were abundant in Yama mice. Immunohistochemistry demonstrated increased expression of eosinophil cationic protein (ECP). Moreover, mRNA expression of Th2 cytokines (IL-4, IL-5, IL-13) and profibrotic mediators (IL-6, Col1a1) was significantly higher in Yama mice. However, the pronounced fibrotic changes, TGF-β expression exhibited only a modest increase in Yama mice, suggesting that fibrosis might develop via pathways not totally dependent on conventional TGF-β signaling. This repeated BLM administration model successfully reproduces the key pathological features of severe IPF and emphasizes the pivotal contribution of eosinophils to fibrogenesis.

Key Words: bleomycin, eosinophil, interstitial pulmonary fibrosis, Yama mice

Introduction

Idiopathic pulmonary fibrosis (IPF) is a chronic and progressive interstitial lung disease with poor prognosis, showing a median survival of 3–5 years[7,8,17,24)]. Patients typically present with dyspnea, cough, and progressive decline in pulmonary function, and its prevalence has been increasing globally, including in Japan[17,18,20,30)]. Experimental models are crucial

* Corresponding author: Masahiro Morimoto
Laboratory of Veterinary Pathology, Joint Faculty of Veterinary Medicine, Yamaguchi University, 1677-1, Yoshida, Yamaguchi 753-8515, Japan.
TEL: +81-839-335-892
FAX: +81-839-335-892
Email: morimasa@yamaguchi-u.ac.jp
doi: 10.57494/jjvr.74.1_1

for understanding fibrotic mechanisms and evaluating potential therapies. Among these, administration of bleomycin (BLM) to the airway is the most commonly used model[18,22,26]. However, the conventional single-dose BLM-induced murine model generally produces only moderate and transient fibrosis, failing to replicate the chronic and progressive remodelling characteristic of human IPF[8,19,22,29].

The pathogenesis of IPF involves repetitive alveolar epithelial injury, aberrant repair processes, and excessive extracellular matrix (ECM) accumulation, ultimately resulting in structural distortion and irreversible lung dysfunction[18,28,31]. While fibrotic lesions with collagen overexpression are defined by histological features, they are not faithfully reproduced in traditional BLM models[12,26,29]. Despite their widespread use in preclinical studies, including evaluations of antifibrotic agents such as nintedanib[5,13,21], existing mouse models remain insufficient.

A novel animal model is needed to more accurately reflect the complex and progressive pathogenesis of IPF[7,8,12,36]. In conventional repetitive BLM administration models, fibrosis can be sustained for a longer period than single-dose protocols; however, several studies have noted that these models still exhibit partial spontaneous resolution and do not fully recapitulate the progressive and irreversible features of human IPF[7,26]. Emerging evidence suggests that eosinophils are involved in fibrosis, and several studies have reported a correlation between eosinophil activity and fibrosis progression[1,2,10]. Eosinophils release profibrotic cytokines such as TGF-β and IL-4, which stimulate fibroblast activation and ECM deposition[3,4,10].

Yama mice possess a unique genetic background characterized by persistent eosinophilia without IL-5 overexpression[34], which has been implicated in tissue remodeling and the amplification of fibrotic responses[35]. This eosinophil-driven milieu may enable Yama mice to develop fibrosis that is more progressive and self-perpetuating than that observed in existing BLM-based models. Importantly, as demonstrated in this study, fibrosis in Yama mice continues to progress even after the final BLM administration, rather than ending ongoing spontaneous resolution. Therefore, Yama mice may provide a more pathophysiology-relevant model for studying the persistent and progressive characteristics of human IPF.

Materials and Methods

Animal models

Male Yama mice maintained in our laboratory and C57BL/6 mice obtained from CLEA Japan, Inc. (Tokyo, Japan) were used (6–8 weeks old). A total of 24 mice were included and randomly divided into four groups (n = 6 per group): C57BL/6-Saline, C57BL/6-BLM, Yama-Saline, and Yama-BLM. The control group was C57BL/6 mice, the most commonly used strain in BLM-induced IPF models. All animals were housed at the Advanced Research Center for Laboratory Animal Science (ARCLAS), Yamaguchi University, under conventional conditions. Environmental parameters were maintained at 24 ± 2 °C and 50–70% humidity, with a 12-hour light/dark cycle. Standard rodent chow (CE-2, CLEA Japan Inc.) and tap water were provided *ad libitum*. All experimental procedures were conducted in accordance with institutional guidelines for animal care and were approved by the Animal Research Committee of Yamaguchi University (Approval Number 589). As part of animal welfare measures, mice exhibiting coughing due to lung injury were euthanized.

Bleomycin administration

Experimental groups received eight intranasal administrations of BLM (2 mg/kg body weight) (Cayman Chemical Co., Ann Arbor, MI, USA) every two weeks, while the control group received saline. The dose of BLM was based on a previous report[26]. The intranasal administration is less invasive and easier to perform repeatedly[27]. All intranasal administrations were performed under anesthesia using a mixture of xylazine 10 mg/kg body weight (Bayer, Tokyo, Japan) and

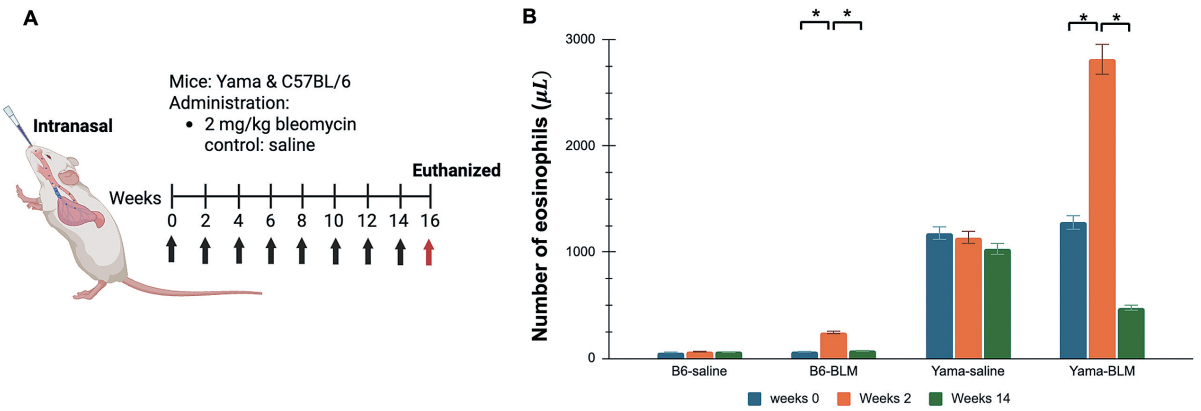

Fig. 1. (A) Schematic illustration of the protocol and research schedule. (B) The number of eosinophils in the peripheral blood before and following the experiment (n = 6). Data are presented as mean ± SD (*$P < 0.05$).

ketamine 80 mg/kg body weight (Daiichi Sankyo Co., Ltd., Tokyo, Japan). All mice were euthanized at the end of the experiment (14 days after the final administration) under anesthesia with a combination of xylazine 10 mg/kg body weight and ketamine 80 mg/kg body weight, with cervical dislocation. The mice were euthanized 14 days after the last BLM administration to analyze the established fibrotic phase, which normally develops after day 14 of the last dose in BLM-induced lung injury, as well as to allow the acute inflammatory reaction to subside[22]. The overall study design is depicted in Fig. 1A.

Peripheral eosinophil count

Following the collection of blood samples one week after each treatment, the samples were then processed using Hinkelmann's staining solution in accordance with previously described procedures[23]. Eosinophils were enumerated manually under a light microscope using a hemocytometer chamber (Erma Sales Co., Ltd., Saitama, Japan).

Histopathological analysis

The left lung lobe was fixed in 10% neutral-buffered formalin and routinely processed for paraffin embedding. Sections (4 μm thick) were stained with hematoxylin and eosin (HE), alcian blue (pH 2.5)–periodic acid–Schiff (AB-PAS), and picrosirius red (PSR) (ScyTek Laboratories, Inc., Logan, UT, USA). PSR staining was used to evaluate collagen deposition, and the percentage of PSR-positive area relative to the total lung area was quantified using ImageJ software (National Institutes of Health, Bethesda, MD, USA). The Ashcroft scoring system was used for determining the severity of fibrosis[6]. Immunohistochemistry was performed using anti-mouse eosinophil cationic protein (ECP) IgG (diluted 1:400; Avicera Bioscience Inc., Santa Clara, CA, USA). A secondary antibody for ECP was used with a goat anti-rabbit polyclonal (Histofine® Simple Stain™ Max PO (R), Nichirei Biosciences Inc, Tokyo, Japan). Antigen retrieval was conducted by incubating tissue sections in 0.1% trypsin for ECP. The number of ECP-positive cells was counted in five randomly selected high-power fields (HPF; 400x magnification; 2.04 mm^2). The histological and quantitative analyses were performed under blinded conditions.

Wet/dry weight ratio assay

The superior lobe lung was excised, rinsed of blood, and weighed immediately. Samples were dried in a drying oven at 60 °C for 72 hr, and the wet/dry weight ratio was calculated. The ratio was calculated as: (W/D ratio) = W (g)/D (g) × 100%[21].

Measurement of hydroxyproline

Hydroxyproline content was quantified using the QuantiChrom™ Hydroxyproline Assay Kit (BioAssay Systems, Hayward, CA, USA) according

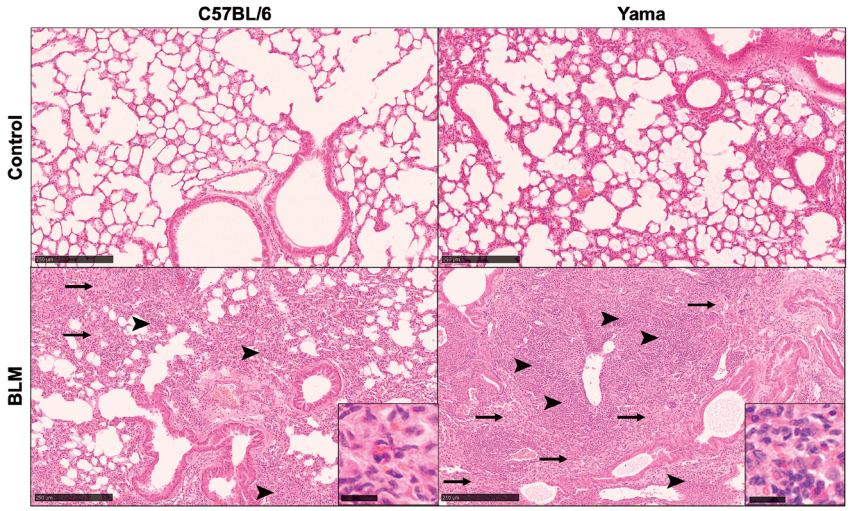

Fig. 2. Histological lung sections from saline-treated and BLM-challenged C57BL/6 and Yama mice stained with hematoxylin and eosin (HE). Saline-treated C57BL/6 and Yama mice exhibit normal alveolar structures with thin septa and minimal inflammation. C57BL/6-BLM mice show moderate interstitial thickening accompanied by inflammatory cell infiltration. Yama-BLM mice display extensive and diffuse septal thickening, alveolar collapse, and dense inflammatory infiltrates. Black arrows indicate interstitial thickening. Black arrowheads indicate inflammatory cell infiltration. Insets highlight eosinophils and neutrophils. Scale bars = 250 μm; inset = 25 μm.

to the manufacturer's instructions. Absorbance was measured at 560 nm using a 2030 Multilabel Reader ARVO X4 (PerkinElmer, Waltham, MA, USA). Hydroxyproline concentrations were determined from a standard curve and expressed as hydroxyproline μg/mL. Collagen conversions were determined 1 μg/mL hydroxyproline is equivalent to 7.69 μg/mL collagen.

Gene mRNA expression analysis

Total RNA was isolated from the remaining frozen lung tissues using RNeasy® Plus Mini Kit (QIAGEN, Tokyo, Japan), in accordance with the manufacturer's protocol. The samples were incubated at 37 °C for 60 min, then subjected to 95 °C for 5 min, and subsequently placed on ice for 5 min to synthesize cDNA using the ReverTra Ace qPCR RT Master Mix (TOYOBO, Osaka, Japan). The target genes comprised interleukin-4 mRNA (IL-4), interleukin-5 mRNA (IL-5), interleukin-6 mRNA (IL-6), interleukin-13 mRNA (IL-13), transforming growth factor-β mRNA (TGF-β), and Col1a1 mRNA. The target genes were quantified with 1 μL of cDNA samples were amplified using TaqMan® Gene Expression Assays (IL-4: Mm00445259-m1, IL-5: Mm00439646-m1, IL-6: Mm0046190-m1, IL-13: Mm00434204-m1, TGF-β: Mm01178820-m1, Col1a1: Mm00801632-gH, Thermo Fisher Scientific Inc., Waltham, MA, USA) and a CFX96 Touch Real-Time PCR Detection system (Biorad Laboratories, CA, USA). The subsequent cycle was performed 60 times for amplification. 95 °C for 1 min; 95 °C for 15 sec; and 60 °C for 1 min. Housekeeping genes (18S rRNA) (Mm03928990-g1, Thermo Fisher Scientific Inc., Waltham, MA, USA) were utilized and standardized with IL-5, IL-4, IL-6, IL-13, TGF-β, and Col1a1. Relative mRNA expression level in the C57BL/6-saline group was used as the baseline.

Statistical analysis

Statistical analyses were performed using JMP Pro software version 15 (SAS Institute, Tokyo, Japan). Data are expressed as mean ± standard deviation (SD). Quantitative data were analyzed using statistical tests following confirmation of normality and homogeneity. Comparisons of peripheral blood eosinophil levels across multiple groups or time points were

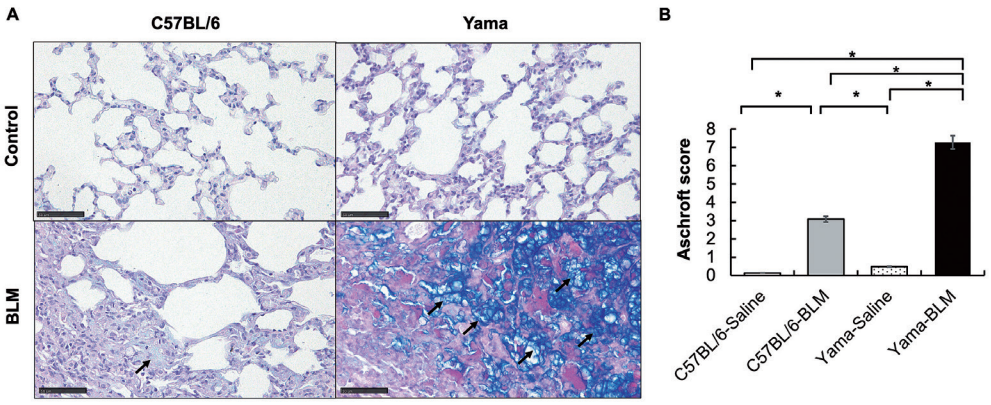

Fig. 3. A. Representation of fibrotic foci via Alcian Blue-Periodic acid-Schiff's (AB-PAS) staining. B. Aschroft score represents C57BL/6 mice and Yama mice (n = 6). Black arrows indicate the fibrotic foci. Data are presented as mean ± SD (**P* < 0.05). Bars = 50 µm.

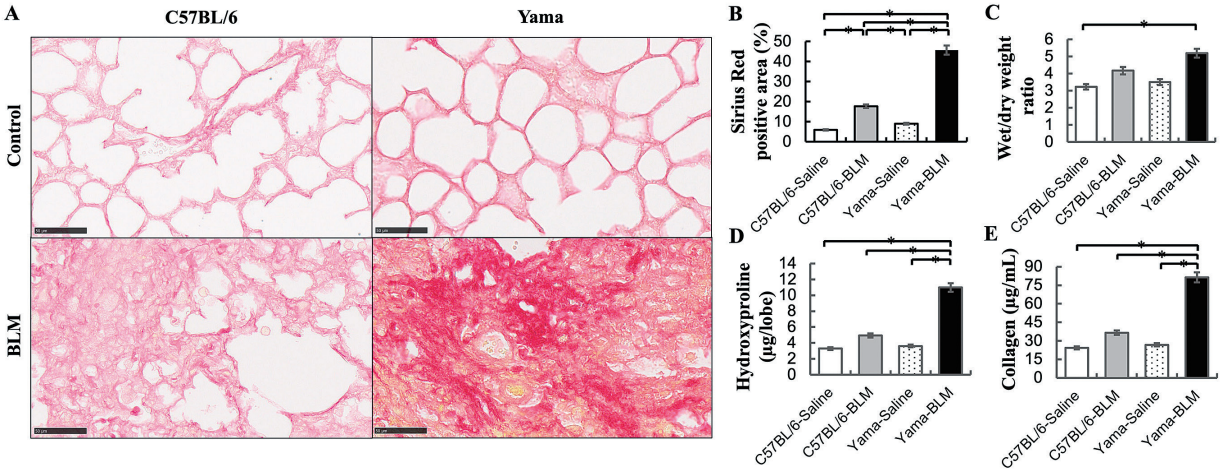

Fig. 4. (A) Representation of Picrosirius red (PSR) staining of the lungs from both Yama and C57BL/6 (BLM-treated as well as controls). (B) Percentage of PSR-positive area. (C) Wet/dry weight lung ratio. (D) Hydroxyproline amount in µg/lobe. (E). Collagen amount in µg/mL. Bars = 50 µm. (n = 6). Data are presented as mean ± SD (**P* < 0.05).

performed using ANOVA followed by Tukey's HSD post hoc test for multiple comparisons. Additionally, comparisons between two groups were conducted using the Student's t-test. A p-value < 0.05 was considered statistically significant.

Results

Peripheral blood eosinophils

At baseline (day 0), Yama mice exhibited significantly higher peripheral blood eosinophil counts compared with C57BL/6 control mice (P < 0.05). Following BLM administration, blood eosinophils were measured biweekly. Yama-BLM mice demonstrated markedly elevated eosinophil counts compared to C57BL/6-BLM mice. In Yama-BLM mice, eosinophil counts peaked at week 2 and gradually decreased toward the end of the examination. In contrast, C57BL/6-BLM mice showed a modest increase at week 2, returning to near baseline levels by the end of the observation period (Fig. 1B).

Histopathological analysis and hydroxyproline content

Histopathological analysis of lung sections from the Yama and C57BL/6 mice stained with HE staining. Both control C57BL/6 and Yama

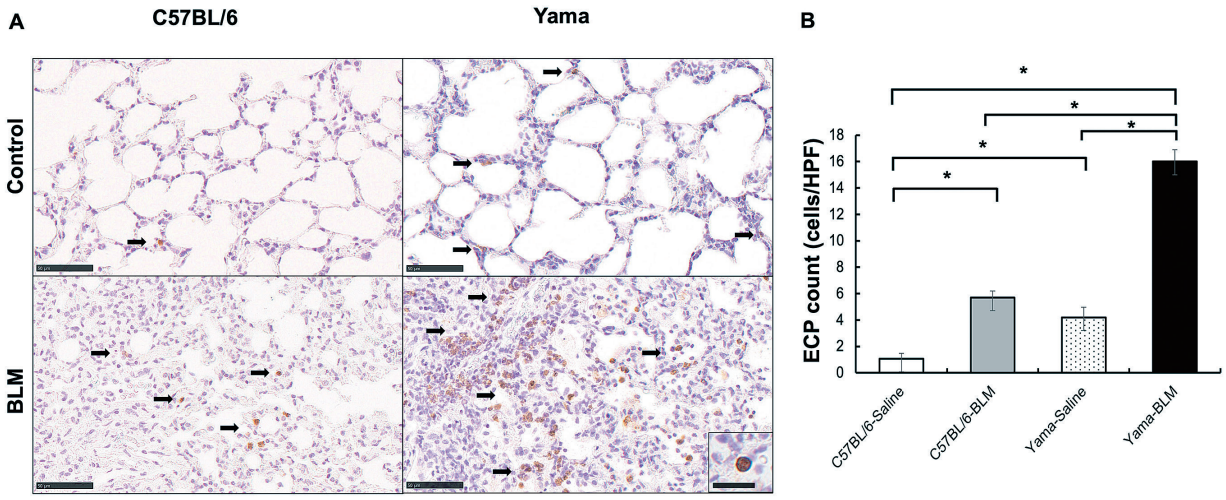

Fig. 5. (A) Representation of eosinophilic cationic protein (ECP) immunohistochemistry of the lungs from both Yama and C57BL/6 mice (BLM-treated as well as controls). Black arrows indicate ECP-positive eosinophils (cytoplasm). Bars = 50 μm. (B) The number of eosinophils in the lung (n = 6; five randomly selected HPF 400x). Data are presented as mean ± SD (*$P < 0.05$).

mice show normal alveolar architecture with thin septa and minimal inflammation. C57BL/6-BLM mice showed moderate interstitial thickening and inflammatory infiltration involving both peribronchiolar and interstitial areas. Yama-BLM mice demonstrate extensive and diffuse pulmonary fibrosis involving both peribronchiolar and interstitial areas, with marked interstitial fibrosis, collapse of alveolar structures, and dense inflammatory cell infiltration (Fig. 2). BLM-treated Yama mice, numerous Alcian blue–PAS-positive fibroblast foci were observed along the alveolar walls. In contrast, the BLM-treated C57BL/6 mice exhibited only a few in fibroblast foci. However, the saline-treated control groups of both strains exhibited minimal to no fibroblast foci (Fig. 3A). Ashcroft's scoring confirmed significantly greater fibrosis severity in Yama mice than C57BL/6 mice (Fig. 3B).

PSR staining revealed significantly greater collagen deposition and collagen-positive area as a percentage of total lung area (%) of the BLM-treated Yama mice, which was consistent with severe fibrotic remodelling. In contrast, the C57BL/6 mice exhibited mild collagen deposition, whereas the saline-treated control groups of both strains demonstrated minimal collagen accumulation (Fig. 4A-B). Yama mice exhibited a greater increase in the wet/dry ratio following BLM administration compared to C57BL/6 mice (Fig. 4C). Hydroxyproline assays further demonstrated that Yama-BLM mice correspond with greater collagen deposition compared with C57BL/6-BLM mice (Fig. 4D-E). Immunohistochemical analysis of ECP revealed marked eosinophil infiltration in the lungs of the BLM-treated Yama mice (Fig. 5A). However, the C57BL/6 group exhibited minimal eosinophil infiltration (Fig. 5B).

Expression of cytokines

Relative mRNA expression level of IL-4, IL-5, IL-6, IL-13, TGF-β, and Col1a1 in the C57BL/6-saline group was used as the baseline. BLM treatment increased IL-4 mRNA expression by 1.31-fold was identified in the C57BL/6-BLM group. Furthermore, the Yama-saline group displayed enhanced relative IL-4 mRNA expression even without treatment (1.45-fold), which increased 2.84-fold upon BLM injection in the Yama-BLM group ($P < 0.05$) (Fig. 6A). Relative IL-5 mRNA expression demonstrated a modest increase in the C57BL/6-BLM group (1.69-fold). The Yama-saline group presented an mRNA expression level comparable to that of the C57BL/6-BLM group (1.77-fold). In contrast, the

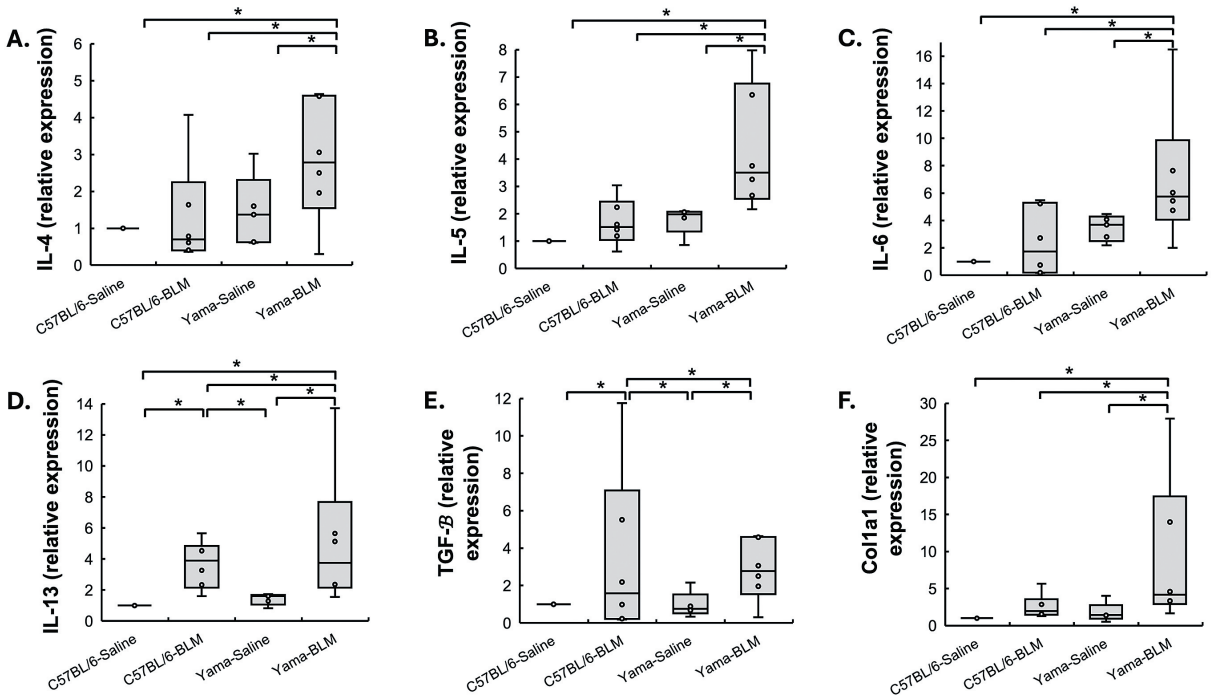

Fig. 6. Relative mRNA expression of interleukin-4 (IL-4) (A), IL-5 (B), IL-6 (C), IL-13 (D), transforming growth factor-β (TGF-β) (E), and Col1a1 (F) in the lungs of both Yama and C57BL/6 mice (n = 6). Data are presented as mean ± SD (*$P < 0.05$).

Yama-BLM group observed a remarkable 4.36-fold increase in IL-5 mRNA expression ($P < 0.05$) (Fig. 6B). IL-6 mRNA expression in the C57BL/6-BLM group exhibited an elevation (2.42-fold). The Yama-saline group already showed an enhanced baseline (3.45-fold), with the largest relative mRNA expression detected in the Yama-BLM group (7.06-fold, $P < 0.05$) (Fig. 6C).

BLM treatment boosted IL-13 mRNA expression in both Yama and C57BL/6 mice, respectively (3.65-fold and 5.13-fold). The Yama-saline group demonstrated a slightly increased mRNA expression 1.42-fold (Fig. 6D). The TGF-β mRNA expression in the C57BL/6-BLM mice was significantly upregulated (3.48-fold, $P < 0.05$). While the Yama-saline group showed slightly lower baseline levels (0.96-fold) and moderate elevation in the Yama-BLM group (2.40-fold) (Fig. 6E). Moreover, the relative Col1a1 mRNA expression was considerably enhanced in the C57BL/6-BLM group (2.54-fold). The relative mRNA expression levels modestly rose in the Yama-saline group (1.78-fold), however a considerable upregulation was found in the Yama-BLM group (9.20-fold, $P < 0.05$) (Fig. 6F).

Discussion

IPF is still one of the most severe interstitial lung diseases, and the therapeutic options remain very limited[5,21]. The prognosis of patients is generally very poor, and therefore, the establishment of animal models that can faithfully reproduce the pathophysiology of IPF is strongly required[13,15,20]. To date, the BLM-induced fibrosis model has been widely used. However, this model is well known to be transient and self-limiting[14,19]. For this reason, it does not reflect the progressive and irreversible fibrosis consistent with the irreversible fibrosis characteristic of human IPF.[19,26,29]. In other words, although the BLM model has contributed to fibrosis research, it still has a fundamental limitation[26,29]. Therefore, the development of new mouse models is necessary.

In the present study, we established a novel

murine model of IPF using Yama mice, which exhibit spontaneous hypereosinophilia[33,34]. Compared with the commonly used C57BL/6 mice, Yama mice showed much higher peripheral eosinophil counts at baseline and sustained eosinophilia after BLM administration[34,35]. The eosinophil levels were likely to have returned to baseline by the end of the study because of eosinophil migration into the airways and infiltration of the lung interstitium. This feature is very important because eosinophils have repeatedly been reported to be related to fibrotic diseases[1–3]. In fact, eosinophil infiltration into damaged lung tissue has been reported in BLM-induced pulmonary fibrosis[2,3,6]. It is known that eosinophils release several fibrogenic cytokines, such as TGF-β1 and IL-4, and also cytotoxic proteins. These mediators aggravate alveolitis and epithelial injury, ultimately promoting tissue remodeling[4,6,10,11].

Therefore, the presence of eosinophilia in Yama mice can explain why they showed more severe fibrosis than C57BL/6 mice. In our experiment, eosinophil counts in Yama mice reached a peak at 2 weeks after BLM treatment and then decreased gradually. This finding is consistent with previous reports that eosinophils act as early responders to lung injury and release pro-fibrotic mediators, which form the basis of subsequent fibrosis[4,6,10]. On the other hand, in C57BL/6 mice, eosinophil mobilization was very limited. This difference between the two strains may be one reason why Yama mice developed more severe fibrotic changes. In summary, it can be said that the inherent eosinophilia of Yama mice is one of the key elements of this model.

Histopathological evaluation also demonstrated that the Yama model reproduces the essential features of human IPF. In Yama mice, the lung exhibited diffuse interstitial thickening, collapse of alveolar structure, and marked infiltration of mononuclear cells and eosinophils[26,27,29,36]. Especially, Alcian blue–PAS–positive fibroblastic foci, which are known as the hallmark lesions of human IPF[36], were abundant in Yama mice but only sporadic in C57BL/6 mice. Furthermore, marked eosinophil infiltration was confirmed by ECP staining, suggesting that immune effector cells and fibroblasts may interact to accelerate fibrosis[1,2,6]. Taken together, these histological findings provide solid evidence that Yama mice reproduce the pathological hallmarks of human IPF.

Biochemical and histological analyses supported these observations. PSR staining and hydroxyproline assay, Yama-BLM mice showed significantly more collagen deposition than C57BL/6-BLM mice. This clearly indicates that the fibrotic process in Yama mice is more aggressive and sustained. Because excessive collagen accumulation is the most important characteristic of human IPF, the present finding strongly suggests that Yama mice more closely reproduce the continuous extracellular matrix remodeling observed in IPF patients[8,13,15].

In addition, the lung wet/dry ratio was also increased in Yama mice. In acute models, such an increase is sometimes interpreted as pulmonary edema[5,21]. However, in the present chronic setting, it is more reasonable to interpret the increase as reflecting a reduction of aerated lung volume and increased parenchymal density caused by collagen accumulation and tissue remodeling[22,25,26]. Thus, both biochemical and physiological findings consistently suggest that Yama mice develop more severe fibrosis than conventional strains.

Cytokine analysis further revealed important mechanistic differences. In Yama mice, IL-4 and IL-5 were elevated at baseline and further increased after BLM treatment. IL-13 was also strongly induced. These cytokines are known as typical Th2 cytokines, and together they promote eosinophilic inflammation, fibroblast activation, and collagen synthesis[2,9,27,32]. In addition, Yama mice showed persistently high IL-6 levels. IL-6 has been reported to stimulates fibroblast proliferation, promotes Th17 responses, and induces epithelial-to-mesenchymal transition[4,9,27,35]. IL-6 elevation is also reported to be associated with poor prognosis in human IPF[18,24]. Therefore, the cytokine environment in Yama mice may mimic the severe phenotype of IPF patients. In summary, Yama mice presented a cytokine profile characterized by a combination

of Th2 dominance and IL-6 elevation, which may explain their severe phenotype.

One particularly interesting finding was the role of TGF-β. In C57BL/6 mice, BLM administration induced strong TGF-β expression, consistent with its well-established function as a key profibrotic cytokine[2,9,16,27]. However, in Yama mice, TGF-β expression increased only moderately despite the presence of more severe fibrosis and marked overexpression of Col1a1. This observation suggests that Yama mice may develop fibrosis through mechanisms that are not entirely dependent on TGF-β signalling. This study did not assess downstream mediators like Smad2/3; however, a previous study indicates that TGF-β signaling may be subject to intrinsic negative-feedback control. The TGF-β promotes rapid activation of Smad3, followed by a gradual downregulation of Smad3 expression in lung fibroblasts, thus limiting further TGF-β signaling[37]. This process may partially figure out how TGF-β mRNA levels in our model exhibit a modest rise despite significant fibrosis. Similar findings, specifically the dissociation between TGF-β signalling and collagen accumulation, have been reported in other Yama-based disease models[35], reinforcing the notion that this strain exhibits a distinct regulatory profile in fibrogenesis.

Therefore, Th2-associated cytokines (e.g., IL-4 and IL-13) and IL-6-driven inflammatory signalling are possibly to serve as major drivers of enhanced fibrotic response in Yama mice. Alternative fibrosis-related pathways—such as Wnt/β-catenin, Notch signalling, and osteopontin[21,28,35] may profoundly contribute to the extensive fibrosis evident in this model and require investigation in upcoming studies. Moreover, the characteristic hypereosinophilic response in Yama mice may create a highly profibrotic tissue microenvironment, facilitated by the release of eosinophil granule proteins, fibroblast activation, and modulation of tissue remodelling, ultimately resulting in more pronounced fibrosis despite the absence of strong TGF-β upregulation. Given that the pathogenic mechanisms of human IPF are heterogeneous, this result increases the translational value of Yama mice. Thus, this model may reflect the diversity of pathogenic mechanisms seen in clinical cases.

In conclusion, Yama mice showed pulmonary fibrosis with severe extracellular matrix deposition, characteristic histological lesions, and a cytokine profile dominated by Th2 and IL-6. In C57BL/6 mice, TGF-β is the main driver of fibrosis, but in Yama mice, immune-related pathways are important. This difference is highly relevant to clinical IPF, because patients' immune signatures vary, and responses to antifibrotic drugs are heterogeneous[5,21]. Therefore, the Yama-BLM model is not only a more severe fibrosis model but also a model reflecting disease heterogeneity. It is a useful platform to investigate noncanonical mechanisms and to test new therapies targeting eosinophil and Th2 pathways. Finally, this model may facilitate identification of therapeutic targets for immune-modulating strategies in preclinical research and thus may contribute to expanding therapeutic options in IPF.

Conflict of Interest

The authors declare that they have no conflicts of interest.

Acknowledgements

This work was supported by JST SPRING, Grant Number JPMJSP2111.

References

1) Aceves SS. Remodeling and fibrosis in chronic eosinophil inflammation. Dig Dis 32, 15–21, 2014. doi: 10.1159/000357004.
2) Adamko D, Spencer LA, Bandeira-Melo-C, Bozza PT, Butterfield JH, Irvin CG, Neves JS, Mahmudi-Azer S, Moqbel R, Weller PF. Eosinophil secretory functions. In: Eosinophils in Health and Disease, Elsevier Inc, USA. pp. 229–275, 2013.

3) Akuthota P, Weller PF. Eosinophils and disease pathogenesis. Semin Hematol 49, 113–119, 2012. doi: 10.1053/j.seminhematol.2012.01.005.
4) Al-muhsen S, Letuve S, Vasquez-Tello A, Pureza MA, Al-Jahdali H, Bahammam AS, Hamid Q, Halwani R. Th17 cytokines induce pro-fibrotic cytokine release from human eosinophils. Respir Res 14, 34, 2013. doi: 10.1186/1465-9921-14-34.
5) Amati F, Stainer A, Polelli V, Mantero M, Gramegna A, Blasi F, Aliberti S. Efficacy of pirfenidone and nintedanib in interstitial lung diseases other than idiopathic pulmonary fibrosis: A systematic review. Int J Mol Sci 24, 7849, 2023. doi: 10.3390/ijms24097849.
6) Cui T, Kusunose M, Hamada A, Ono M, Miyamura M, Yoshioka S, Kyotani S, Nishioka Y. Relationship between the eosinophilia of bronchoalveolar lavage fluid (BALF) and the severity of pulmonary fibrosis induced by bleomycin in rats. Bio Pharm Bull 26, 959–963, 2003. doi: 10.1248/bpb.26.959.
7) Degryse Al, Tanjore H, Xu XC, Polosukhin VV, Jones BR, McMahon FB, Gleaves LA, Blackwell TS, Lawson WE. Repetitive intratracheal bleomycin models several features of idiopathic pulmonary fibrosis. Am J Physiol Lung Cell Mol Physiol 299, 442–452, 2010. doi: 10.1152/ajplung.00026.2010.
8) Degryse AL, Lawson WE. Progress toward improving animal models for IPF. Am J Med Sci 341, 444-449, 2011. doi: 10.1097/MAJ.0b013e31821aa000.
9) Franzen L, Lindvall MO, Huhn M, Ptasinski V, Setyo L, Keith BP, Collin A, Oag S, Volckaert T, Borde A, Lundeberg J, Lindgren J, Belfield G, Jackson S, Ollerstam A, Stamou M, Stahl PL, Hornberg JJ. Mapping spatially resolved transcriptomes in human and mouse pulmonary fibrosis. Nat Genet 56, 1725–1736, 2024. doi: 10.1038/s41588-024-01819-2.
10) Fulkerson PC, Rothenberg ME. Targeting eosinophils in allergy, inflammation and beyond. Nat Rev Drug Discov, 12, 117–129, 2023. doi: 10.1038/nrd3838.
11) Gharaee KM, Phan SH. The role of eosinophils in pulmonary fibrosis (review). Int J Mol Med 1, 43–53, 1998. doi: 10.3892/ijmm.1.1.43.
12) Gul A, Yang F, Xie C, Du W, Mohammadtursun N, Wang B, Le J, Dong, J. Pulmonary fibrosis model of mice induced by different administration methods of bleomycin. BMC Pulm Med 23, 91, 2023. doi: 10.1186/s12890-023-02349-z.
13) Guo H, Sun J, Zhang S, Nie Y, Zhou S, Zeng Y. Progress in understanding and treating idiopathic pulmonary fibrosis: recent insights and emerging therapies. Front Pharmacol 14, 1205948, 2023. doi: 10.3389/fphar.2023.1205948.
14) Herrera JA, Dingle LA, Monetero A, Venkateswaran RV, Blaikley JF, Granato F, Pearson S, Lawless C, Thornton DJ. Morphologically intact airways in lung fibrosis have an abnormal proteome. Respir Res 24, 99, 2023. doi: 10.1186/s12931-023-02400-x.
15) Hutchinson J, Fogarty A, Hubbard R, McKeever T. Global incidence and mortality of idiopathic pulmonary fibrosis: a systematic review. Eur Respir J 46, 795–806, 2015. doi: 10.1183/09031936.00185114.
16) Kliment CR, Englert JM, Crum LP, Oury TD. A novel method for accurate collagen and biochemical assessment of pulmonary tissue utilizing one animal. Int J Clin Exp Pathol 4, 349–355, 2011.
17) Kondoh Y, Suda T, Hongo Y, Yoshida M, Hiroi S, Iwasaki K, Takeshima T, Homma S. Prevalence of idiopathic pulmonary fibrosis in Japan based on a claims database analysis. Respir Res 23, 24, 2022. doi: 10.1186/s12931-022-01938-6.
18) Lederer DJ, Martinez FJ. Idiopathic pulmonary fibrosis. N Engl J Med 378, 1811–1823, 2018. doi: 10.1056/NEJMra1705751.
19) Lee JU, Nam, Y, Baek J, Park E, Hong J, Choi YM, Kim SH, Jeong SH, Kim WJ, Park SW. Progressive lung fibrosis in aged mice induced by repetitive bleomycin: Exacerbation by long-term PM2.5 inhalation. Ecotoxicol Environ Saf 304, 119146, 2025. doi: 10.1016/j.ecoenv.2025.119146.
20) Ley B, Collard, HR, King-Jr TE. Clinical

course and prediction of survival in idiopathic pulmonary fibrosis. Am J Respir Crit Care Med 183, 431–440, 2011. doi: 10.1164/rccm.201006-0894CI.

21) Miao Y, Wang Y, Bi Z, Huang K, Gao J, Li X, Li S, Wei L, Zhou H, Yang C. Antifibrotic mechanism of avitinib in bleomycin-induced pulmonary fibrosis in mice. BMC Pulm Med 23, 94, 2023. doi: 10.1186/s12890-023-02385-9.
22) Moore BB, Hogaboam CM. Murine models of pulmonary fibrosis. Am J Physiol Lung Cell Mol Physiol 294, 152–160, 2008. doi: 10.1152/ajplung.00313.2007.
23) Morimoto M, Yamada M, Arizono N, Hayashi T. Lactic dehydrogenase virus infection enhances parasite egg production and inhibits eosinophil and mast cell responses in mice infected with the nematode Nippostrongylus brasiliensis. Immunology 93, 540–545, 1998. doi: 10.1046/j.1365-2567.1998.00454.x.
24) Raghu G, Chen SY, Hou Q, Yeh WS, Collard HR. Incidence and prevalence of idiopathic pulmonary fibrosis in US adults 18–64 years old. Eur Respir J 48, 179–186, 2016. doi: 10.1183/13993003.01653-2015.
25) Raghu G, Remy-Jardin M, Myers JL, Richeldi L, Ryerson CJ, Lederer DJ, Behr J, Cottin V, Danoff SK, Morell F, Flaherty KR, Wells A, Martinez FJ, Azuma A, Bice TJ, Bouros D, Brown KK, Collard HR, Duggal A, Galvin L, Inoue Y, Jenkins RG, Johkoh T, Kazerooni EA, Kitaichi M, Knight SL, Mansour G, Nicholson AG, Pipavath SNJ, Buendia-Roldan I, Selman M, Travis WD, Walsh SLF, Wilson KC. Diagnosis of idiopathic pulmonary fibrosis. An official ATS/ERS/JRS/ALAT clinical practice guideline. Am J Respir Crit Care Med 198, e44–e68, 2018. doi: 10.1164/rccm.201807-1255ST.
26) Redente EF, Black BP, Backos DS, Bahadur AN, Humpries SM, Lynch DA, Tuder RM, Zemans RL, Riches DWH. Persistent, progressive pulmonary fibrosis and epithelial remodeling in mice. Am J Respir Cell Mol Biol 64, 669–676, 2021. doi: 10.1165/rcmb.2020-0542MA.
27) Santa AZ, Ognjenovic A, Antolic M, Cuzic S, Glojnaric I, Hrvacic B, Bozic F. Retrospective assessment of nintedanib in the mice model of pulmonary fibrosis: alignment with patient outcomes in idiopathic pulmonary fibrosis. Veterinarska Stanica 54, 395–406, 2023. doi: 10.46419/vs.54.4.4.
28) She YX, Yu QY, Tang XX. Role of interleukins in the pathogenesis of pulmonary fibrosis. Cell Death Discov 7, 52, 2021. doi: 10.1038/s41420-021-00437-9.
29) Song S, Fu Z, Guan R, Zhao J, Yang P, Li Y, Yin H, Lai Y, Gong G, Zhao S, Yu J, Peng X, He Y, Luo Y, Zhong N, Su J. Intracellular hydroxyproline imprinting following resolution of bleomycin-induced pulmonary fibrosis. Eur Respir J 59, 2100864, 2022. doi: 10.1183/13993003.00864-2021.
30) Wang J, Zhu F, Liu Y, Luo R, Fan Z, Dai W, Wei S, Lin C. A novel mouse model of pulmonary fibrosis: twice-repeated oropharyngeal bleomycin administration mimicking human pathology. Biochem Cell Biol 103, 1–7, 2025. doi: 10.1139/bcb-2024-0221.
31) Wijsenbeek M, Cottin V. Spectrum of fibrotic lung diseases. N Engl J Med 383, 958–968, 2020. doi: 10.1056/NEJMra2005230.
32) Wolters PJ, Collard HR, Jones KD. Pathogenesis of idiopathic pulmonary fibrosis. Annu Rev Pathol 9, 157–179, 2013. doi: 10.1146/annurev-pathol-012513-104706.
33) Xu M, Zhao C, Song H, Wang C, Li H, Qiu X, Jing H, Zhuang W. Inhibitory effects of Scisandrin C on collagen behaviour in pulmonary fibrosis. Sci Rep 13, 13475, 2023. doi: 10.1038/s41598-023-40631-6.
34) Yamada Y, Okamoto K, Kagimoto S, Sakurai M, Sakai Y, Hasegawa M, Imai H, Shibutani S, Morimoto M. Establishment of mutant mouse strain showing eosinophilia. Scandinavian Journal of Laboratory Animal Science 51, 1–8, 2025. doi: 10.23675/sjlas.v51i.24006.
35) Yamada Y, Yoshizaki K, Sakurai M, Morimoto M. Establishment of new mouse model for allergic dermatitis showing severe fibrosis. J Vet Med Sci 86, 1303–1310, 2024. doi: 10.1292/jvms.24-0394.

36) Yamaguchi M, Hirai S, Tanaka Y, Sumi T, Miyajima M, Mishina T, Yamada G, Otsuka M, Hasegawa T, Kojima T, Niki T, Watanabe A, Takahashi H, Sakuma Y. Fibroblastic foci, covered with alveolar epithelia exhibiting epithelial-mesenchymal transition, destroy alveolar septa by disrupting blood flow in idiopathic pulmonary fibrosis. Lab Invest 97, 232–242, 2017. doi: 10.1038/labinvest.2016.135.
37) Zhao Y, Geverd DA. Regulation of Smad3 expression in bleomycin-induced pulmonary fibrosis: a negative feedback loop of TGF-β signaling. Biochem Biophys Res Commun 294, 319–323, 2002. doi: 10.1016/S0006-291X(02)00471-0.
38) Zhen Z, Peng F, Zhou Y. Biomarkers in idiopathic pulmonary fibrosis: Current insight and future direction. Chin Med J Pulm Crit Care Med 2, 72–79, 2024. doi: 10.1016/j.pccm.2024.04.003.